Downregulation of HBx Restrains Proliferation, Migration and Invasion of HepG2 Cells

Chaoqun Huang
The 962nd Hospital of the PLA
Wei Liu
The 962nd Hospital of the PLA
Xiaochuan Zhao
The 962nd Hospital of the PLA
Libin Zhao
The 962nd Hospital of the PLA
Fuxiang Wang (✉ Fuxiangwang3261@163.com)
The Third People's Hospital of Shenzhen https://orcid.org/0000-0002-7687-5415

Research

Keywords: Liver cancer, Hepatic B virus X protein, XB130, HepG2 cells, Proliferation, PI3K/AKT signaling

Posted Date: June 19th, 2020

DOI: https://doi.org/10.21203/rs.3.rs-36398/v1

Version of Record: A version of this preprint was published at Analytical Cellular Pathology on May 13th, 2021. See the published version at https://doi.org/10.1155/2021/6615979.

Abstract

Background: Liver cancer is a frequent malignancy with high fatality. Hepatic B virus X protein (HBx) could promote theprogression of liver cancer. Meanwhile, aberrantly expressed XB130 was identified in liver cancer. However, relevant molecular mechanism is poorly studied. Our present study mainly investigated the mechanism of liver cancer.

Methods: After microarray-based analyses in liver cancer tissues and the matched adjacent normal tissues, upregulated mRNA was screened out. Contents of HBx and XB130 in liver cancer tissues as well as cells HepG2 were examined by reverse transcription quantitative polymerase chain reaction (RT-qPCR) and Western blot analysis. Correlation between HBx and XB130 was analyzed in HepG2 cells, followed by verification by RIP assay. After gain- and loss-of-function experiments, cellular proliferation, invasion, migration and colony formation ability were assessed using CCK-8, Transwell, wound healing experiment and colony formation assay.

Results: Both HBx and XB130 expression was elevated in liver cancer, which was correlated with poor survival rate of liver cancer patients. Moreover, HBx and XB130 were positively correlated in HepG2 cells. RIP assay verified that HBx could bind to XB130. Loss of HBx hindered proliferation, and migration/invasion of HepG2 cells but promoted apoptosis, which was partially reversed by overexpressed XB130.

Conclusion: The conclusion reached from the study offered an understanding of the role of HBx/XB130 played in liver cancer. Our study first reported the regulatory relation between HBx and XB130, which may be valuable to discover therapeutic targets for liver cancer treatment.

Introduction

Based on the estimation by American Cancer Society, liver cancer is a prevalent cancer with rapidly increased incidence [1]. Also, the survival rate of liver cancer is comparatively low, for instance, 20% in United Kingdom, with high incidence worldwide [2]. Based on global study, there were over 700,000 cases of liver cancer in 2012, among which 56% cases were induced by hepatitis B virus (HBV) and 20 by hepatitis C virus [3]. Burgeoning studies have revealed that HBV plays a crucial role in development of liver cancer [4, 5]. HBV is a hepadnaviridae family member, which is currently regarded as the smallest animal virus with diameter of 42 nm and spherically shaped [6]. Furthermore, HBV X protein (HBx) is closely related to the infection of HBV [7]. However, evidence on the mechanism by which HBx mediates liver cancer is limited, which warrants further study.

HBx is found to be initiated at the integration of HBV DNA into the genome of the hepatocytes, which is often detected in the malignant hepatocytes [8]. Moreover, HBx is associated with liver cancer pathogenesis since HBx could mediate specific proto-oncogenes at transcriptional level, yet the detailed mechanism of HBx remains to be further investigated [9]. Correlation of HBx with liver cancer has been studied since inhibition of HBx possesses the potential to alleviate HBV-infected liver cancer [10]. Our

study attempted to further the study on impacts of HBx on liver cancer progression. Additionally, aberrant expression of XB130 is further linked to the tumor classification, lymph node metastasis, and prognosis in various kinds of cancers [11]. Also, mRNA expression of XB130 is identified in common human cancers involving liver cancer [12]. Further exploration reveals that XB130 is correlated with the activation of the PI3K/AKT pathway in liver cancer [13]. The PI3K/AKT pathway is associated with the biological functions of liver cancer cells [14]. Specifically, the PI3K/AKT signaling pathway could promote cell proliferation in liver cancer [15]. The current study focused on the axis of the HBx/XB130/PI3K/AKT pathway in liver cancer, accompanied with examination of the progression of liver cancer. To our best knowledge, the present study is the first to illustrate the binding relation between HBx and XB130 in liver cancer. Our study is expected to reveal a new mechanism for occurrence of HBx-related liver cancer.

Materials And Methods

Study object

A total of 63 patients with liver cancer hospitalized in The 962nd Hospital of the PLA from January 2014 to January 2016 were included in this study. All included patients met the following criteria: 1. without history of combined chronic diseases; 2. without history of chemotherapy or physical therapy before surgery in The 962nd Hospital of the PLA; 3. without family history of related tumors. Based on the 7th edition of the Union for International Cancer Control (UICC) tumor lymph node metastasis (TNM) staging standard (2010), patients were classified. All surgically resected liver cancer tissues and adjacent normal tissues (more than 5 cm away from cancerous tissues) were rapidly stored in liquid nitrogen at -80℃. Detailed information for patients is listed in Table 1.

Table 1
The clinical feature of liver cancer patients

Clinicopathological features		Cases (n)
Sex	Male	35
	Female	28
Age (years)	≤ 60	41
	> 60	22
Tumor size	≤ 5 cm	36
	> 5 cm	27
Venous infiltration	Yes	36
	No	17
Metastasis	Yes	40
	No	21

Microarray-based analysis

Microarray-based analyses were performed using Affymetrix. RNA was extracted from tissues with TRIzol reagent (Thermo Fisher Scientific, USA) and hybridized with GeneChip Human Gene 2.0 ST Array (Thermo Fisher Scientific) at 48℃ and 60 rpm, which was then washed and stained followed by scanning with a GeneChipTM Scanner 3000 7G system (Thermo Fisher Scientific). Data analysis was subsequently carried out using Expression Console Software with background correction and normalization of raw data by robust multichip analysis (RMA, City of Industry, CA, USA). mRNAs with differential expression were identified according to *t*-test. The heatmap of differential mRNAs was plotted with $p < 0.01$ and |Fold change| > 2 as threshold.

Experimental antibodies

The following antibodies were used in this study: primary antibodies against HBx (ab39716, dilution at 1:500 for Western blot analysis; 1:100 for RNA Binding Protein Immunoprecipitation (RIP) assay; 1:200 for Immunohistochemistry (IHC); Abcam, Cambridge, UK), XB130 (#12684, dilution at 1:1000 for Western blot analysis; 1:50 for RIP; 1:100 for IHC; Cell Signaling Technology, Boston, MA, USA), AKT (#9272, 1:1000, Cell Signaling Technology), phosphorylated-AKT (Ser473) (#4060, 1:2000, Cell Signaling Technology), and β-actin (sc-47778; 1:500, Santa Cruz, CA, USA) as well as a secondary antibody (ab205718, 1:10000, Abcam).

IHC

The obtained liver tissue samples were fixed in 4% paraformaldehyde for 1 h and embedded in dehydrated paraffin. Tissues were then sectioned and immersed with blocked permeable solution for 30 min, which were the incubated with 3% hydrogen peroxide for 10 min and blocked by 5% goat serum. A total of 50 μL primary antibody was added into the sections for an incubation for 1 h at room temperature, followed by an incubation of secondary antibody for 30 min at 37℃. Next, sections were added with 50 μL peroxidase, and the color was developed with Diaminobenzidine (DAB) for 5 min. Washed by phosphate buffers saline (PBS), tissue sections were counterstained with hematoxylin. After 30 s of differentiation with ethanol hydrochloride, the cells were dehydrated, mounted and observed under an inverted microscope (IX53, Olympus, Tokyo, Japan).

Cell culture and transfection

Human liver cancer cell line HepG2 and normal hepatocyte MIHA were incubated in Roswell Park Memorial Institute-1640 medium at 37℃ with 5% CO_2. The cell suspension of HepG2 cells was cultured in a 37℃ incubator with 5% CO_2 for 24 h, after which cells were seeded onto culture dishes for overnight culture. The plasmids containing small interfering RNA targeting HBx (si-HBx) and XB130 (si-XB130) fragments and empty plasmids were transfected into HepG2 cells using Lipofectamine 2000 (Thermo Fisher Scientific) when cell confluence reached 60%. At 4 h post-transfection, the medium was renewed, and cells were further incubated for 48 h for subsequent experiments. The pcDNA3.1 plasmids

(GenePharma, Shanghai, China) were used, while the sequence fragments were synthesized by Sangon Biotechnology (Shanghai, China).

Western blot analysis

Cells were dissolved on ice in Radioimmunoprecipitation assay buffer (50 mmol/L Tris-Cl [pH = 7.5], 120 mmol/L NaCl, 10 mmol/L NaF, 10 mmol/L sodium pyrophosphate, 2 mmol/L ethylenediaminetetraacetic acid, 1 mmol/L Na_3VO_4, 1 mmol/L phenylmethylsulfonyl fluoride, and 1% NP-40) containing proteinase inhibitor cocktail (Roche, Basel, Switzerland). The protein content of the cleavage products was measured by bicinchoninic acid. A total of 30 μg of protein was separated by 8% sodium dodecyl sulfate-polyacrylamide gel electrophoresis (SDS-PAGE) and transferred to a polyvinylidene fluoride (Millipore, Bedford, MA, USA) membrane, which was blocked with 5% bovine serum albumin (BSA) after marker separation. Subsequently, the membrane was incubated with the above-mentioned primary antibodies at 4°C for 16 h, and then with secondary antibody at room temperature for 1 h. Immunoreactive protein bands were determined using enhanced chemiluminescence system (Thermo Fisher Scientific, USA), which were quantified by QuantityOne v4.6.2 imaging software (Bio-Rad, USA).

Reverse transcription quantitative polymerase chain reaction (RT-qPCR)

Total RNA from tissues and cells was extracted with TRIzol reagent (Thermo Fisher Scientific, USA), followed with measurement of quality and concentration of RNA by a NanoDrop ND1000 spectrophotometer (Thermo Fisher Scientific). RNA was reversely transcribed into complementary DNA (cDNA) using the miRcute miRNA cDNA first-strand synthesis kit (Tiangen Biotech Co., Ltd., Beijing, China). Quantitative PCR was performed using the SYBR-Green I Master Mix kit (Thermo Fisher Scientific), whereas PCR was performed in the GeneAmp PCR system (PE2400, USA). The results of electrophoresis were scanned by an ultraviolet peroxide with Gel Doc 100 gel detector (Bio-Rad), with gray values of each band calculated by Image J software. Primers for HBx and XB130 (Table 2) were synthesized by GenePharma (Shanghai, China).

Table 2
Primer sequences for RT-qPCR

Gene	Sequences
XB130	F: 5'-CGGACTCAGACUCUTGCCUTU-3'
	R: 5'-CUGUAGCTUACCGTTGUUCG-3'
HBx	F: 5'-ACCGACCTTGAGGCCTACTT-3'
	R: 5'-GCTTGGCAGAGGTGAAAG-3'
GAPDH	F: 5'-GACCTGACCTGCCGTCTA-3'
	R: 5'-AGGAGTGGGTGTCGCTGT-3'

Notes: RT-qPCR, Reverse transcription quantitative polymerase chain reaction; GAPDH, glyceraldehyde-3-phosphate dehydrogenase

RIP

For Co-IP analysis, HepG2 cells were lysed by incubation with protein G-agarose beads (Roche Diagnostics, Switzerland) at 4℃ for 1 h, followed with cell centrifugation. The collected supernatant was incubated overnight at 4℃ with 4 μg anti-HBx antibody or immunoglobulin G (IgG; Thermo Fisher Scientific). The immune complexes were precipitated by incubation with 50 μL protein G-agarose at 4℃ for 3 h. Agarose beads were precipitated by centrifugation and washed three times with lysis buffer. Next, the beads were suspended in 2 × Laemmli sample buffer (Sigma-Aldrich) for 5 min. The protein G-agarose beads were removed from the complex by a 10,000 g centrifugation for 5 min, and the supernatant was loaded onto 10% SDS-PAGE for Western blot analysis.

Cell counting kit (CCK)-8 assay

Cells were seeded on 96-well plates containing 100 μL Dulbecco's modified eagle medium (DMEM) at a density of 3×10^3 cells/well. After 24, 48 and 72 h of incubation at 37℃ and 5% CO_2, the original medium was discarded and a DMEM containing 10 μL CCK8 solution (Takara, Japan) was added. After another 3 h of incubation, the optical density (OD) value of cells at 450 nm was measured using a microplate reader RT-6100 (Rayto, Shenzhen, China), and the growth curve was plotted.

Colony formation assay

A total of 5,000 cells were mixed with 0.5% soft agar (Solarbio, Beijing, China), which were added to a 6-well plate covered with 0.8% agar. The top of the agar was added with 2 mL complete medium, followed by cell culture in standard culture environment for 2 weeks. Afterwards, colonies were photographed and counted under an inverted microscope (IX53, Olympus).

Wound healing experiment

Cells at 90% confluence were seeded into a 6-well plate and cultured overnight at 37℃ with 5% CO_2. Wounds with interval of 5 mm were made using a pipette along the layer of adherent cells. The cells within the scratch were removed by PBS, and fresh medium was added to further the culture. Cell migration to wound was evaluated by photographing at 0 and 24 h.

Transwell assay

The invasive ability of HepG2 cells was evaluated by Transwell assay. Cells (5×10^4 cells) were seeded in 0.5 mL serum-free medium and then added to the apical Transwell chamber, while 0.75 mL medium containing 5% fetal bovine serum added to the basolateral chamber. The Transwell chamber was incubated for 18 h and fixed with 4% paraformaldehyde for 1 h, followed by the removal of cell debris and addition of hematoxylin (BD Biosciences, San Jose, CA, USA) for a 1-h staining at room temperature. Cells were photographed under a microscope (IX53, Olympus) with five visual fields randomly selected.

Flow cytometry for detection of cellular apoptosis

Cell apoptosis was assessed using Annexin V-fluorescein isothiocyanate (FITC)/propidium iodide (PI) apoptosis detection kits (Solarbio). Briefly, cells were detached with 0.25% trypsin, resuspended in PBS with 1×10^6 cells/mL, and fixed with 0.7 mL absolute ethanol for 24 h. After a centrifugation at 180 g for 30 s, the supernatant was discarded. Cells were resuspended in 1 mL PBS followed by another centrifugation. The precipitated cells were suspended with 100 μL 1 mg/mL RNase A, and the cell suspension was incubated with 400 μL 50 μg/mL Annexin V-FITC for 15 min in the dark. Following that, 400 μL 50 μg/mL PI was added into cells and incubated for 10 min in void of light. The cellular apoptosis was determined by a flow cytometer (CytoFLEX, BECKMAN COULTER).

Flow cytometry for detection of cellular cycle

Cells in logarithmic growth phase were collected and seeded in a 6-well plate at 1×10^5 cells/well, which were cultured overnight at 37℃ with 5% CO_2. After trypsinization, cells were collected and centrifuged in a flow tube at 1,000 r/min for 5 min. Following addition of 70% precooled ethanol, the precipitates were fixed at 4℃ for more than 18 h, and then added with RNAase (50 mg/L) at 10 μL/well and PI (50 mg/L) at 300 μL/well under shaking. After 30 min of reaction at room temperature in void of light, DNA detection was performed by a flow cytometer (CytoFLEX, BECKMAN COULTER), and the proportion of cell cycle in each phase was analyzed by Modifit software (Verity Software House, USA).

Statistical analysis

The SPSS22.0 (IBM SPSS Statistics, Chicago, IL, USA) was employed for statistical analysis. Measurement data derived from repeated independent experiments were expressed as mean ± standard deviation. Survival analysis was performed as by means of Kaplan-Meier analysis, while unpaired *t*-test was used for comparison between two groups. One-way or two-way analysis of variance (ANOVA) and Tukey's post-test were used for data comparison among multiple groups, and log rank test was used for statistical post-analysis, with $p < 0.05$ as the indicator of statistical significance.

Results

HBx and XB130 are upregulated in liver cancer patients

The samples of liver cancer tissues and adjacent normal tissues were obtained from liver cancer patients. Moreover, 4 patients at stage T1 to T4 were selected, respectively, followed by extraction of total RNA from liver cancer tissues and adjacent normal tissues for microarray-based analysis. It was found that the expression of HBx and XB130 in liver cancer tissues were the most significantly upregulated (foldchange values higher than 10) (Fig. 1A). Therefore, HBx and XB130 expression in liver cancer tissues was further studied. Our results showed that HBx and XB130 expression was upregulated in cancer tissues of all enrolled liver patients (Fig. 1B-C) and positively correlated with the tumor size (Fig. 1D-E). In order to further detect the protein levels of HBx and XB130 in liver cancer tissues, IHC staining was performed, results of which displayed that the positive rates of HBx and XB130 in liver cancer tissues were much higher than those in adjacent normal tissues (Fig. 1F). Subsequently, HBx and XB130 were used as markers to analyze the prognosis of liver cancer patients. The patients were grouped by the median expression of HBx and XB130, respectively. Patients with low expression of HBx and XB130 showed higher survival rate after surgery (Fig. 1G-H).

HBx and XB130 are aberrantly expressed in HepG2 cells

Expression of HBx and XB130 in both HepG2 cells and normal hepatocytes MIHA was further explored. It was shown that both HBx and XB130 were highly expressed in HepG2 cells compared with the MIHA cells (Fig. 2A). Western blot analysis also revealed that the protein levels of HBx and XB130 were increased in HepG2 cells in contrast to MIHA cells (Fig. 2B). The results indicated that HBx and XB130 may play a promoting role in the development of liver cancer. Therefore, HepG2 cells were transfected with pcDNA 3.1 plasmid containing si-HBx or XB130-OE, and HBx/XB130 expression in cells was quantified by PCR to select the cells with the highest efficiency, that is, the cells with the lowest expression of HBx and the highest expression of XB130 for subsequent experiments (Fig. 2C-D).

HBx binds to XB130 in HepG2 cells

Next, we investigated the binding relation between HBx and XB130 in HepG2 cells. Among HepG2 cells overexpressing XB130, HBx expression did not significantly change. However, in cells silencing HBx, XB130 level was reduced (Fig. 3A). The protein levels of XB130 and HBx were similar to the results we observed in Fig. 3A (Fig. 3B). Correlation of the HBx with XB130 expression was analyzed in liver cancer tissues, which showed that HBx was positively correlated with XB130 (Fig. 3C). The binding of HBx to XB130 was further detected, which displayed that enrichment of XB130 in cells with low expression of HBx was significantly reduced (Fig. 3D). These results indicated that HBx might bind to XB130 in HepG2 cells to affect the cellular activity.

Downregulation of HBx attenuates proliferation of HepG2 cells, which can be partially restored by XB130

Subsequently, HBx expression was silenced while XB130 was overexpressed simultaneously in HepG2 cells (Fig. 4A), and stably transfected HepG2 cells were cultured for 0, 24, 48, and 72 h, respectively, followed by observation of the OD value at 450 nm by CCK8 assay. After 72 h, the OD value of cells with low expression of HBx decreased distinctly. In contrast, the OD value of cells co-transfected with XB130 was elevated, indicating enhanced proliferation ability (Fig. 4B). Meanwhile, colony formation of cells was observed, in which the number of cell colony formation was reduced after HBx was silenced, whilst simultaneously overexpressed XB130 increased the number of cell colony formation (Fig. 4C). These experiments suggested that the downregulation of HBx reduced the proliferation ability and cell activity of HepG2 cells, while increase of XB130 expression partially reversed the inhibiting effects of depleted HBx on cell proliferation.

Loss of HBx suppresses migration/invasion of HepG2 cells

Wounds (5 mm long) were made in HepG2 cells which were cultured for 24 h, followed by observation of the distance of wound healing. The distance between the wounds was significantly wider in HepG2 cells silencing HBx than that in untreated HepG2 cells, while the upregulation of XB130 in the presence of HBx knockdown led to the opposite result (Fig. 5A). Transwell assay revealed that the number of invasive cells was lessened after HBx was downregulated, which was partially increased after XB130 was upregulated (Fig. 5B), indicating that depletion of HBx inhibited cell migration and invasion, while XB130 could reverse the inhibiting effect of HBx on cell migration and invasion.

Depletion of HBx promotes apoptosis of HepG2 cells

To further detect the effect of downregulated HBx on HepG2 cell apoptosis, flow cytometry was conducted, the results of which showed that low expression of HBx increased the percentage of positive cells, yet further overexpressed XB130 reduced cell apoptosis (Fig. 6A). Th cell cycle was further examined, and it was found that poor expression of HBx arrested more cells in G0/G1 phase but less cells in the S phase, accompanied with basically unchanged G2/M phase. However, further overexpressed XB130 promoted cells arrested in G0/G1 phase entering into the S phase (Fig. 6B), which indicated that downregulation of HBx increased the apoptotic number of HepG2 cells, while XB130 curtailed the apoptotic activity of cells.

HBx blocks the PI3K/AKT pathway via **XB130**

The extent of AKT phosphorylation (Ser 473) was detected in MIHA and HepG2 cells by Western blot analysis. Results showed that the extent of AKT phosphorylation in HepG2 cells was increased. Moreover, it was found that the downregulation of HBx reduced the extent of AKT phosphorylation in HepG2 cells,

which was partially restored after overexpression of XB130. The above results indicated that the activity of PI3K/AKT pathway was elevated in HepG2 cells and could be mediated by HBx/XB130 (Fig. 7).

Discussion

HBV has been suggested to significantly induce liver cancer [16]. However, the underlying regulatory mechanism of HBV-infected liver cancer has not been fully elaborated. The present study was conducted in a bid to explore HBx-regulated mechanism in liver cancer, in which we collected clinical liver cancer tissues and relevant adjacent normal tissues and purchased liver cancer cell line HepG2, since HepG2 cells are the most frequently used cell line for studies on liver cancer [17].

According to the microarray-based study, we found that HBx and XB130 were remarkably upregulated, which was consistent with our further detection of HBx and XB130 expression in liver cancer tissues and cells. As prior work revealed, highly expressed HBx has been found in HepG2 cells, which contributes to hepatocarcinogenesis [18]. Moreover, HBx accelerates the progression of liver cancer induced by HBV infection [19]. Our study also exhibited that patients with low expression of HBx had a higher survival rate, which was consistent with prior study reporting that upregulated HBx predicts poor prognosis of liver cancer [20]. Meanwhile, XB130 overexpression has also been identified. XB130 is deemed as a predictor for gastric cancer, since XB130 is highly expressed in gastric cancer [21]. Consistent with our study, XB130 is also overly expressed in liver cancer, suggesting that XB130 may be indicative of the diagnosis of liver cancer [13]. Moreover, it is demonstrated that the positive rate of XB130 in a total of 64 liver cancer patients is 75%, yet the comparison of XB130 expression between cancer tissues and adjacent normal tissues was not presented, nor did the detailed molecular mechanism underlying XB130 [22]. All the above cited literature cooperatively supports our findings that HBx and XB130 were upregulated in liver cancer, which may play an oncogenic role in liver cancer.

Subsequent investigation explored the regulatory relationship between HBx and XB130 in liver cancer. HepG2 cells were transfected with pcDNA 3.1 plasmids with altered expression of HBx or XB130. Our results of western blot analysis, correlation study and RIP assay together indicated that HBx bound to and positively regulated expression of XB130 in liver cancer. As far as we concerned, the analysis on binding relation between HBx and XB130 was rare. However, the binding of HBx with other adaptor proteins has been reported before. For instance, HBx could bind to cellular damaged DNA binding protein 1 which is an adaptor protein for the cullin 4A Really Interesting New Gene E3 ubiquitin ligase complex [23]. XB130 is also reported to be an adaptor protein with controversial effects on cancers, since expression of XB130 differs depending on types of cancers [11]. Thus, an in-depth investigation on the role of XB130 in liver cancer is required in our future study. Our mechanistic analysis further showed that HBx mediated the PI3K/AKT pathway *via* XB130. It has been documented that XB130 knockdown could impair the PI3K/AKT pathway in liver cancer to increase the apoptosis of liver cancer cells [13]. Furthermore, another study proves that the activation of the PI3K/AKT pathway is dependent on upregulated HBx [20]. We then furthered our study on the impacts of HBx/XB130/PI3K/AKT pathway on biological function of HepG2 cells. Results of CCK-8, Transwell, wound healing experiment and colony

formation assay suggested that HBx promoted proliferation, migration and invasion of HepG2 cells but inhibited the cell apoptosis by activating XB130-mediated PI3K/AKT pathway. These results validated our statement that HBx and XB130 accelerated progression of liver cancer *in vitro* in association with the PI3K/AKT pathway.

Conclusion

Conclusively, this study proposed high expression of HBx/XB130 in liver cancer. Moreover, downregulation of HBx/XB130 can affect properties of liver cancer HepG2 cells, arresting cells in the G0/G1 phase (Fig. 8). Furthermore, overexpression of XB130 can partially reversed the inhibiting effects of depleted HBx on cells, which provided a target for the pathogenesis of liver cancer. However, the downstream mechanism underlying the PI3K/AKT pathway may also exist, which needs further study. Moreover, an *in vivo* assay is needed to further verify our findings derived from *in vitro* experiments. Nevertheless, the current study presents a novel mechanism for HBV-related liver cancer and may assist to substantiate novel therapeutic approaches.

Abbreviations

ANOVA
Analysis of variance; BCA:Bicinchoninic Acid; BSA:Bovine serum albumin; CCK-8:Cell counting kit-8; cDNA:complementary DNA; DAB:Diaminobenzidine; DMEM:Dulbecco's modified eagle medium; FITC:Fluorescein isothiocyanate; GAPDH:Glyceraldehyde-3-phosphate dehydrogenase; HBx:Hepatic B virus X protein; IgG:Immunoglobulin G; IHC:Immunohistochemistry; OD:optical density; PBS:Phosphate buffers saline; PI:Propidium iodide; PVDF:Polyvinylidene Fluoride; RIP:RNA Binding Protein Immunoprecipitation; RPMI:Roswell Park Memorial Institute; RT-qPCR:Reverse transcription quantitative polymerase chain reaction; SDS-PAGE:Sodium dodecyl sulfate-polyacrylamide gel electrophoresis; TNM:Tumor lymph node metastasis; UICC:The Union for International Cancer Control; UVP:Ultraviolet peroxide; WMA:World Medical Association.

Declarations

Ethics approval and consent to participate

All the study protocol followed the *Declaration of Helsinki* and subsequent amendments published by the World Medical Association (WMA) in 1964. All patients provided the signed informed consent, and the experimental procedures were ratified by the Ethics Committee of The 962nd Hospital of the PLA.

Consent for publication

Not applicable.

Availability of data and materials

All the data generated or analyzed during this study are included in this published article.

Competing interests

The authors declare that they have no competing interests.

Funding

This work was supported by Outstanding Youth Program of Heilongjiang Natural Science Foundation (YQ2019H035).

Authors' contributions

CQHconceived the study and participated in its design and coordination; CQH, WL, XCZ, LBZ and FXW performed all experiments; CQH and FXW analyzed and interpreted the data; The draft was improved through discussion and editing by all the authors who read and approved the final manuscript.

Acknowledgments

The authors would like to thankOutstanding Youth Program of Heilongjiang Natural Science Foundation (YQ2019H035).

References

1. Siegel RL, Miller KD, Jemal A. Cancer statistics, 2020. CA Cancer J Clin. 2020;70(1):7–30.
2. Gravitz L. Liver cancer. Nature. 2014;516(7529):1.
3. Maucort-Boulch D, de Martel C, Franceschi S, Plummer M. Fraction and incidence of liver cancer attributable to hepatitis B and C viruses worldwide. Int J Cancer. 2018;142(12):2471–7.
4. Eller C, Heydmann L, Colpitts CC, El Saghire H, Piccioni F, Juhling F, et al. A genome-wide gain-of-function screen identifies CDKN2C as a HBV host factor. Nat Commun. 2020;11(1):2707.
5. Xie G, Wang X, Wei R, Wang J, Zhao A, Chen T, et al. Serum metabolite profiles are associated with the presence of advanced liver fibrosis in Chinese patients with chronic hepatitis B viral infection. BMC Med. 2020;18(1):144.
6. Karayiannis P. Hepatitis. B virus: virology, molecular biology, life cycle and intrahepatic spread. Hepatol Int. 2017;11(6):500–8.
7. Ling LR, Zheng DH, Zhang ZY, Xie WH, Huang YH, Chen ZX, et al. Effect of HBx on inflammation and mitochondrial oxidative stress in mouse hepatocytes. Oncol Lett. 2020;19(4):2861–9.
8. Zhang XD, Wang Y, Ye LH. Hepatitis B virus X protein accelerates the development of hepatoma. Cancer Biol Med. 2014;11(3):182–90.
9. Ye Y, Yang J, Hu Q, Mao J, Yang Q, Chen H, et al. SIP1 serves a role in HBxinduced liver cancer growth and metastasis. Int J Oncol. 2019;55(5):1019–32.

10. Chen YY, Wang WH, Che L, Lan Y, Zhang LY, Zhan DL, et al. BNIP3L-Dependent Mitophagy Promotes HBx-Induced Cancer Stemness of Hepatocellular Carcinoma Cells via Glycolysis Metabolism Reprogramming. Cancers (Basel). 2020;12(3).
11. Shiozaki A, Kosuga T, Ichikawa D, Komatsu S, Fujiwara H, Okamoto K, et al. XB130 as an independent prognostic factor in human esophageal squamous cell carcinoma. Ann Surg Oncol. 2013;20(9):3140–50.
12. Zhang R, Zhang J, Wu Q, Meng F, Liu C. XB130: A novel adaptor protein in cancer signal transduction. Biomed Rep. 2016;4(3):300–6.
13. Li GM, Liang CJ, Zhang DX, Zhang LJ, Wu JX, Xu YC. XB130 Knockdown Inhibits the Proliferation, Invasiveness, and Metastasis of Hepatocellular Carcinoma Cells and Sensitizes them to TRAIL-Induced Apoptosis. Chin Med J (Engl). 2018;131(19):2320–31.
14. Chen L, Liu D, Yi X, Qi L, Tian X, Sun B, et al. The novel miR-1269b-regulated protein SVEP1 induces hepatocellular carcinoma proliferation and metastasis likely through the PI3K/Akt pathway. Cell Death Dis. 2020;11(5):320.
15. Bamodu OA, Chang HL, Ong JR, Lee WH, Yeh CT, Tsai JT. Elevated PDK1 Expression Drives PI3K/AKT/MTOR Signaling Promotes Radiation-Resistant and Dedifferentiated Phenotype of Hepatocellular Carcinoma. Cells. 2020;9(3).
16. Torresi J, Tran BM, Christiansen D, Earnest-Silveira L, Schwab RHM, Vincan E. HBV-related hepatocarcinogenesis: the role of signalling pathways and innovative ex vivo research models. BMC Cancer. 2019;19(1):707.
17. Yin L, Xia Y, Xu P, Zheng W, Gao Y, Xie F, et al. Veratramine suppresses human HepG2 liver cancer cell growth in vitro and in vivo by inducing autophagic cell death. Oncol Rep. 2020.
18. Arzumanyan A, Friedman T, Ng IO, Clayton MM, Lian Z, Feitelson MA. Does the hepatitis B antigen HBx promote the appearance of liver cancer stem cells? Cancer Res. 2011;71(10):3701–8.
19. Lee YM, Kim S, Park RY, Kim YS. Hepatitis B Virus-X Downregulates Expression of Selenium Binding Protein 1. Viruses. 2020;12(5).
20. Liu YC, Lu LF, Li CJ, Sun NK, Guo JY, Huang YH, et al. Hepatitis B Virus X Protein Induces RHAMM-Dependent Motility in Hepatocellular Carcinoma Cells via PI3K-Akt-Oct-1 Signaling. Mol Cancer Res. 2020;18(3):375–89.
21. Shi M, Huang W, Lin L, Zheng D, Zuo Q, Wang L, et al. Silencing of XB130 is associated with both the prognosis and chemosensitivity of gastric cancer. PLoS One. 2012;7(8):e41660.
22. Zuo Q, Huang H, Shi M, Zhang F, Sun J, Bin J, et al. Multivariate analysis of several molecular markers and clinicopathological features in postoperative prognosis of hepatocellular carcinoma. Anat Rec (Hoboken). 2012;295(3):423–31.
23. Minor MM, Hollinger FB, McNees AL, Jung SY, Jain A, Hyser JM, et al. Hepatitis B Virus HBx Protein Mediates the Degradation of Host Restriction Factors through the Cullin 4 DDB1 E3 Ubiquitin Ligase Complex. Cells. 2020;9(4).

Figures

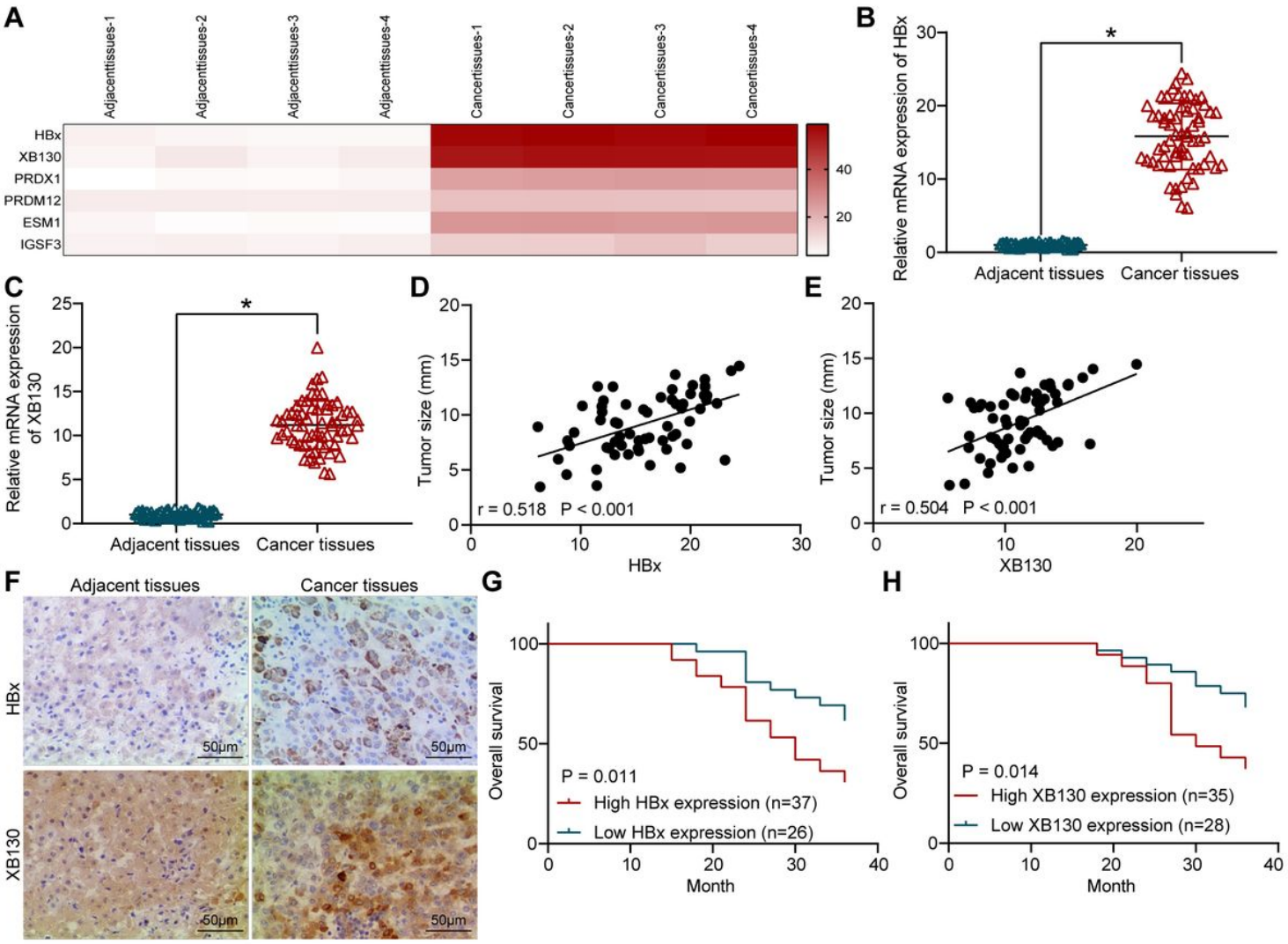

Figure 1

Expression of HBx and XB130 in liver cancer tissues and the matched adjacent normal tissues. A, Differential mRNAs in liver cancer tissues and adjacent normal tissues screened out using microarray-based analyses. B-C, Expression of HBx and XB130 in liver cancer and adjacent normal tissues examined by RT-qPCR. D-E, Correlation analysis on HBx and XB130 with tumor size. F, Contents of HBx and XB130 in tissues analyzed by IHC. G-H, Survival analysis on HBx and XB130 expression with prognosis of liver cancer patients. * p< 0.01 indicates statistical significance.

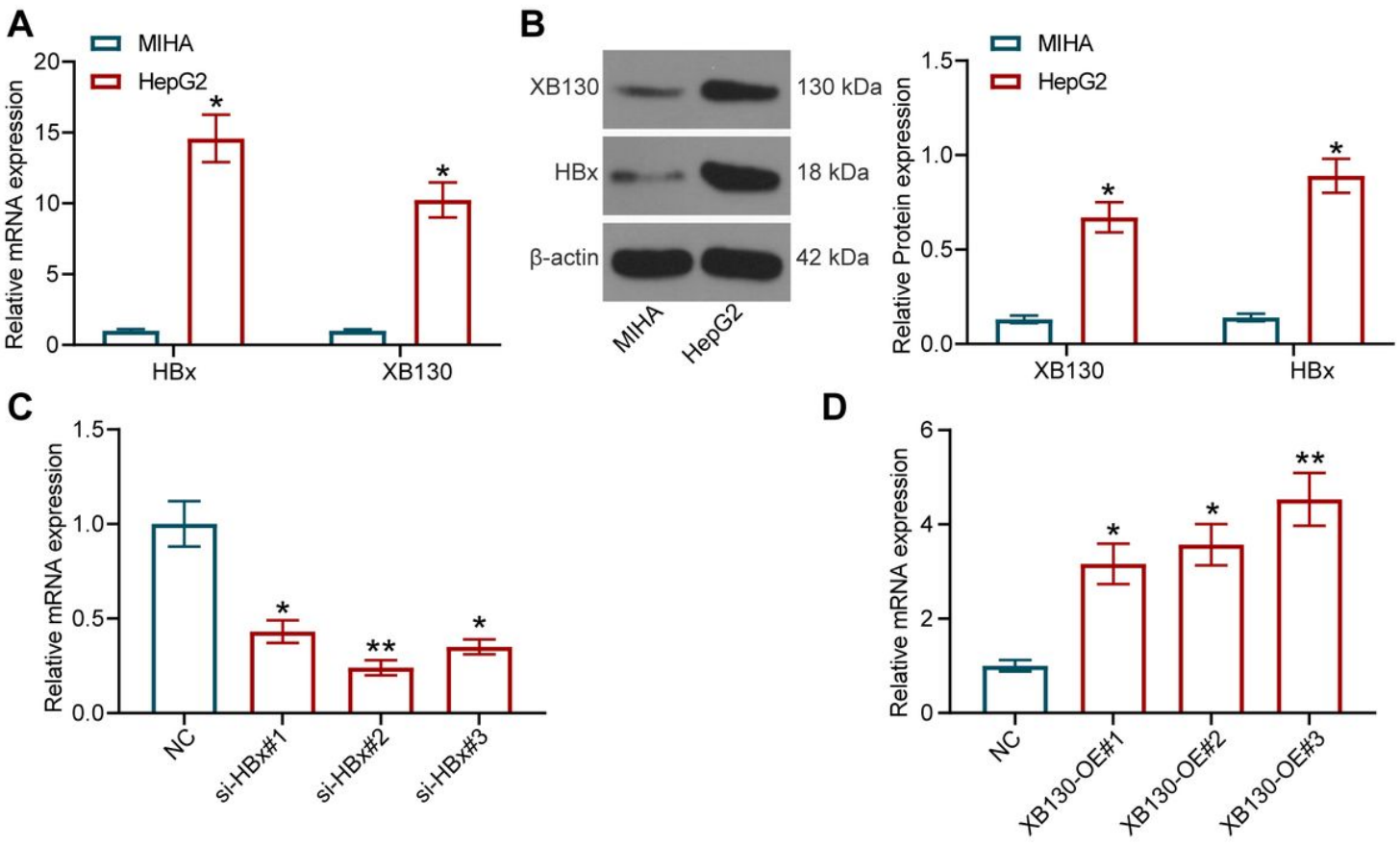

Figure 2

Expression of HBx/XB130 in liver cancer cells and normal hepatocytes. A, Expression of HBx/XB130 in HepG2 and MIHA cells determined by RT-qPCR. B, Protein levels of HBx/XB130 in HepG2 and MIHA cells analyzed by Western blot analysis. C-D, Transfection efficiency of pcDNA 3.1 plasmids containing si-HBx or XB130-OE evaluated by RT-qPCR. * p< 0.01, ** p < 0.01.

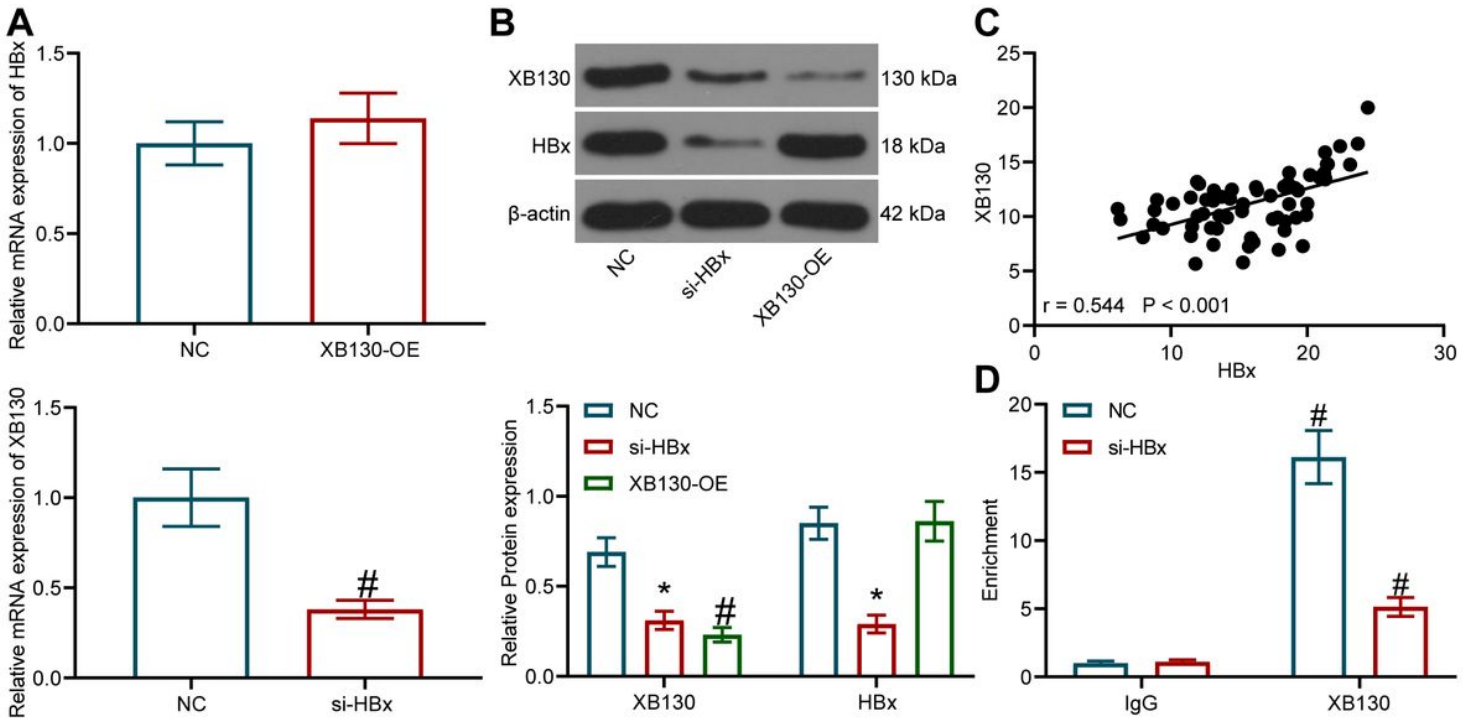

Figure 3

Binding relation of HBx with XB130 in HepG2 cells. A-B, Protein and mRNA expression of HBx and XB130 in HepG2 cells with high expression of XB130 and low expression of HBx determined by RT-qPCR and Western blot analysis. C, Correlation relation of XB130 with HBx in liver cancer tissues. D, Binding relation between HBx and XB130 analyzed by RIP. * indicates that HBx expression is significantly different. # indicates that XB130 expression is significantly different.

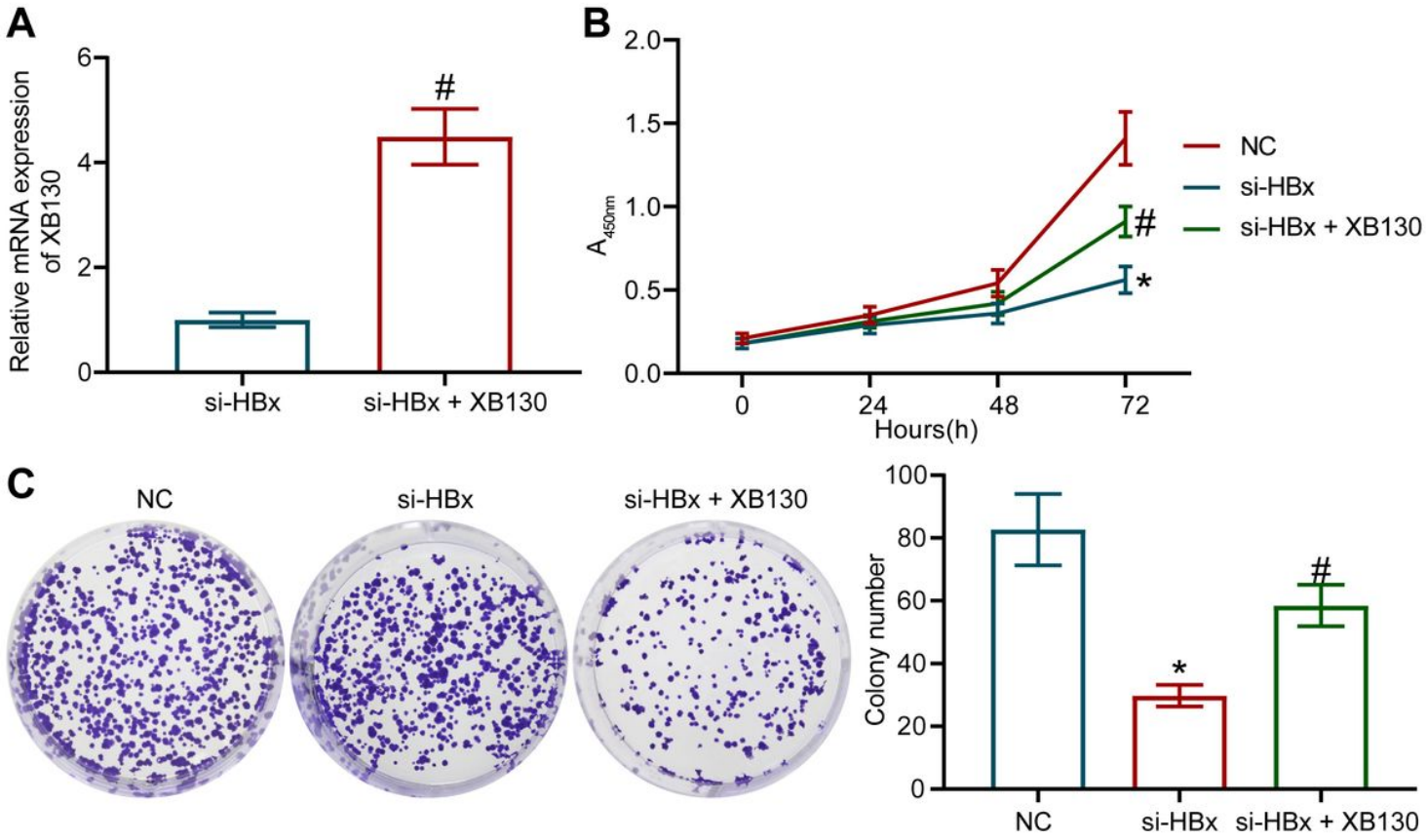

Figure 4

HBx/XB130 axis facilitates proliferation of HepG2 cells. A, Transfection efficiency of cells with silenced HBx and overexpressed XB130 detected by RT-qPCR. B, Proliferative ability of cells examined by CCK-8 assay. C, Colony formation ability of cells examined by colony formation assay. * indicates the difference between NC and si-HBx is significantly different. # indicates the difference between si-HBx and si-HBx + XB130 is significantly different.

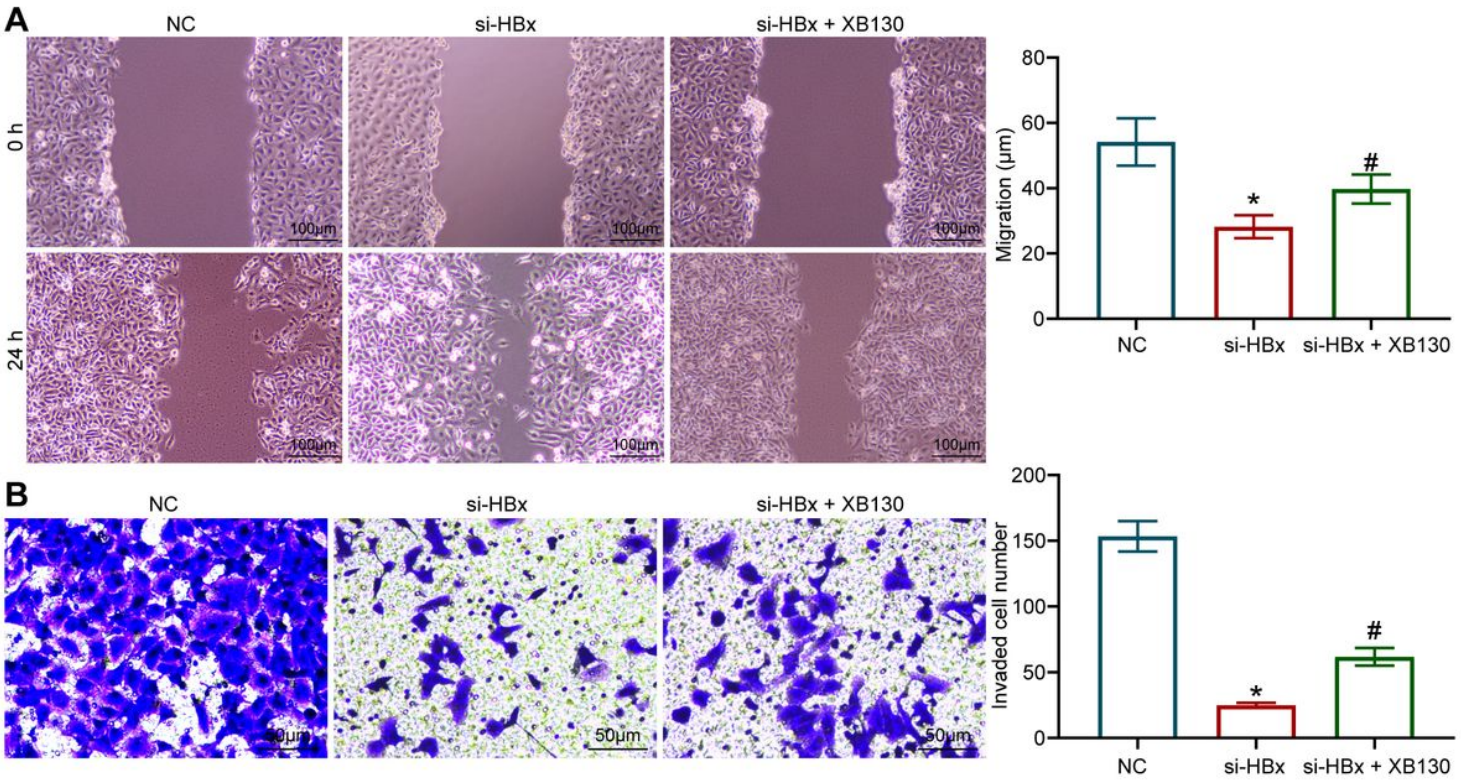

Figure 5

HBx promotes migration/invasion of HepG2 cells by upregulating XB130. A, cellular migrationassessed by wound healing assays. B, Number of invasive cells determined by Transwell assay. * indicates the difference between NC and si-HBx is significantly different. # indicates the difference between si-HBx and si-HBx + XB130 is significantly different.

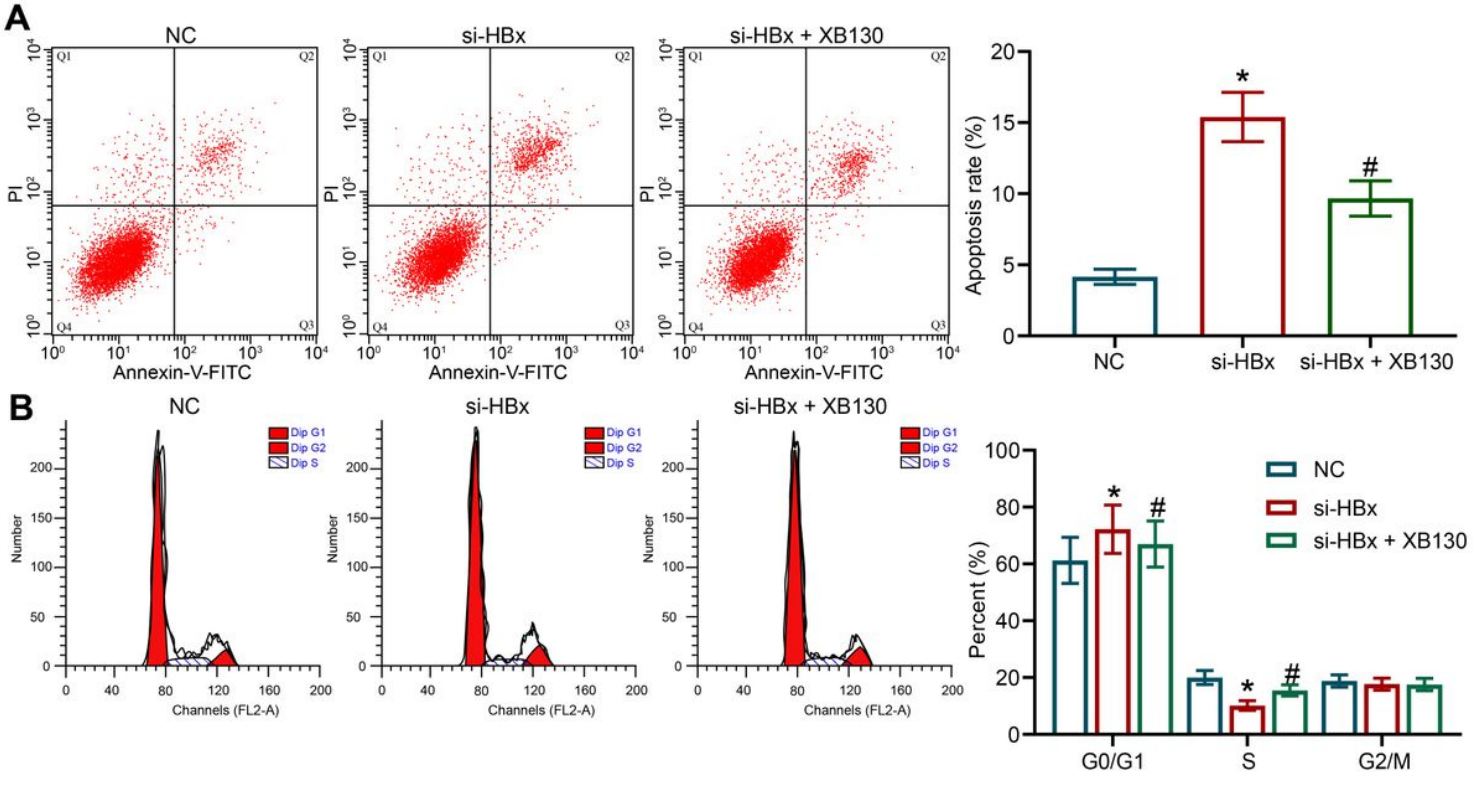

Figure 6

HBx suppresses apoptosis of HepG2 cells by increasing XB130 expression. A, Cell apoptosis examined using flow cytometry. B, Cell cycle determined using flow cytometry. * indicates the difference between NC and si-HBx is significantly different. # indicates the difference between si-HBx and si-HBx + XB130 is significantly different.

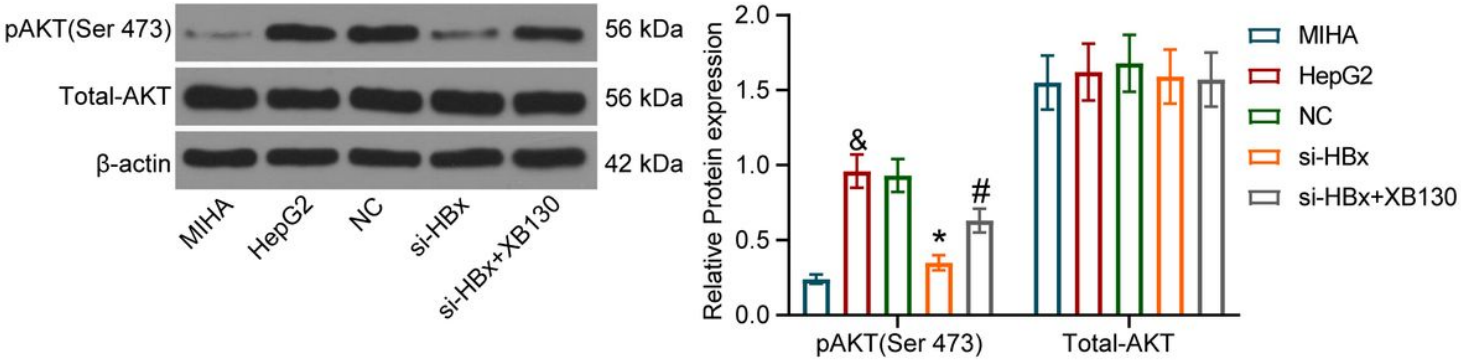

Figure 7

HBx activates the PI3K/AKT pathway by upregulating XB130, which is determined by western blot analysis.

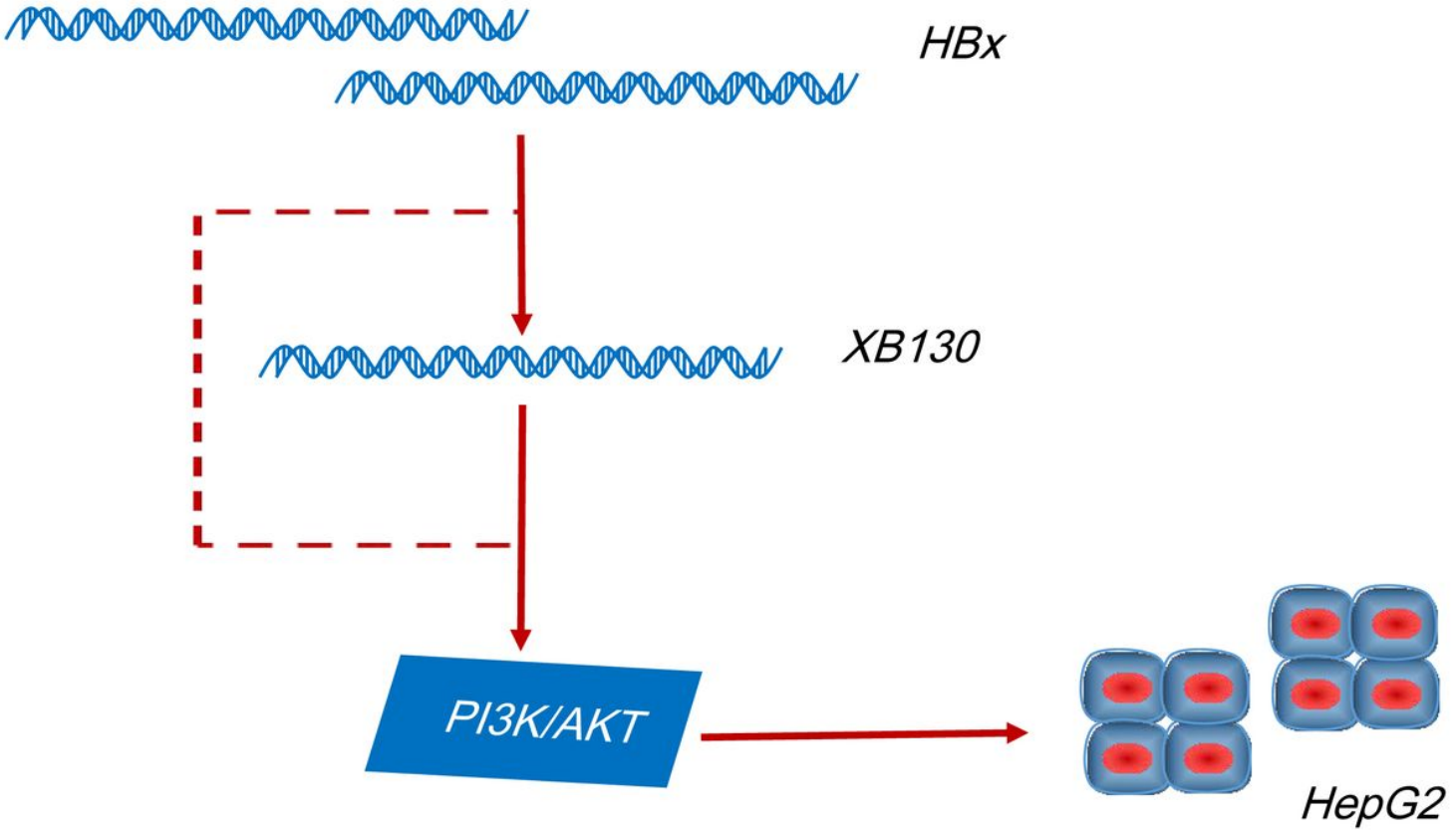

Figure 8

Schematized analysis showing that HBx promotes activity of PI3K/AKT pathway by binding to XB130, which enhanced proliferation, migrationand invasion of HepG2 cells and curtailed cellular apoptosis.